Carbon Nanofiber Paper and Its Effect on Cure Kinetics of Low Temperature Epoxy Resin

Siva Movva,[1] Xilian Ouyang,[1] Jose Castro,[2] L. James Lee[1,2]

[1]*Department of Chemical and Biomolecular Engineering, Koffolt Laboratories, The Ohio State University, Columbus, Ohio 43210*
[2]*Department of Integrated Systems Engineering, Koffolt Laboratories, The Ohio State University, Columbus, Ohio 43210*

Received 6 May 2011; accepted 4 November 2011
DOI 10.1002/app.36437
Published online 20 January 2012 in Wiley Online Library (wileyonlinelibrary.com).

ABSTRACT: In this study, the preparation, properties, and characterization of thin films or "nanopapers" of carbon nanofibers (CNFs) were studied. Specifically, a layer-by-layer nanopaper preparation method was used, which significantly improved the mechanical properties of nanopapers. The effect of CNF nanopaper on the cure kinetics of a low temperature epoxy resin was studied. A modified autocatalytic model was used to represent the reaction kinetics. It was found that the presence of CNF nanopaper substantially increased the resin reaction rate and final conversion.
 J Appl Polym Sci 125: 2223–2230, 2012

Key words: nanoparticle; differential scanning calorimetry (DSC); mechanical properties; modeling

INTRODUCTION

The development of paper-like films made of nanoparticles has attracted much attention in the past decade because of its potential applications in catalysis, filtration, sensors, actuators, super-capacitors, artificial muscles, hydrogen storage materials, and anode materials in lithium ion batteries.[1] These films, also called nanopapers, are typically produced using dispersion and filtration of a suspension of nanoparticles.[2,3] Most studies have concentrated on using single walled and multiwalled carbon nanotubes (CNTs).[4–9] While CNTs have exceptional inherent properties, they are also very expensive. To meet the needs of various challenging applications at a reduced cost, carbon nanofibers (CNFs) have gained a great deal of attention in industry because they have very good inherent properties like CNTs and they are affordable. However, there have been very few studies regarding CNF nanopapers in the literature.

CNF nanopapers are a viable option for use as structural and functional coatings in epoxy composites for various applications, including lightweight coating materials for electromagnetic interference shielding; lightning strike and abrasion protection of various structures, such as aircraft, automobiles, and wind turbine blades. In this study, a layer-by-layer approach was used with the conventional suction filtration method to prepare multilayered nanopapers. This multiple layered approach could be used to incorporate similar nanoparticles of opposite charge, or different nanoparticles in each layer to introduce multifunctionality in the paper. The multilayered CNF nanopapers prepared in this study showed a significant improvement in strength over a commercially available CNF nanopaper. Sancaktar et al.[10] studied the effect of CNF mat on the cure kinetics of epoxy resins. However, the CNF content used in their study was less than 5 wt %, similar to most of the bulk-mixed epoxy/CNF nanocomposites. Here, we used CNF nanopapers with 25 wt % particle loading to study the reaction kinetics of epoxy/CNF nanopaper.

Correspondence to: J. Lee (lee.31@osu.edu).

Journal of Applied Polymer Science, Vol. 125, 2223–2230 (2012)

EXPERIMENTAL

Materials

An epoxy resin, EPIKOTE™ RIM 135 with an epoxy equivalent weight (EEW) of about 166–185, and a diamine curing agent, EPIKURE™ RIM H 137 with an amine value of about 400–600 mg [KOH]/g, were provided by Hexion Specialty Chemicals (Houston, TX). This is a low temperature and low viscosity resin designed especially for manufacturing wind turbine blades. CNFs (PR-24-XT-LHT-OX) were obtained from Applied Sciences (Cedarville, OH). A 50% aqueous solution of Polyethyleneimine (PEI) (molecular weight $M_n \sim$ 50,000–60,000) from Fisher Scientific (Pittsburgh, PA) was used in the amine functionalization of the CNFs. *N*,*N*-Dimethylformamide (DMF) was used as the solvent in this reaction.

Nitric acid ACS reagent (70%) and sulfuric acid (98%) purchased from Fisher Scientific were used for the carboxyl functionalization of the CNFs. For making nanopapers, a highly hydrophilic polycarbonate membrane filter with a pore size of 0.4 μm was purchased from Millipore (Billerica, MA).

Procedures and instrumentation

For preparing the nanopapers, a vacuum filtration technique was used. In this set up, a 90 mm diameter glass filter holder with a stainless steel screen membrane support was placed over a conical flask. Once the membrane filter was placed in the set up and clamped, it was connected to a vacuum aspirator pump. The nanoparticle solution was prepared as follows: a 0.1 wt % aqueous solution of CNFs was sonicated using a Branson digital sonifier at 85% amplitude for 30 min. The resulting solution was cooled down to room temperature in a refrigerator and then filtered through the filtration set up previously described under a pressure of $\sim$ 400 KPa. Vacuum was applied for about 30 min after all the water was filtered away. The nanopapers were dried overnight at room temperature and then stored in airtight containers. This process was repeated several times for multilayered papers.

Mechanical properties of the nanopapers were measured using a Rheometrics Solids Analyzer (RSA-III) from TA Instruments. Tensile tests were conducted on $\sim$ 5 mm wide samples at a gauge length of 10 mm. Digital Vernier calipers were used to measure the individual width and thickness of each nanopaper. A minimum of three readings were taken in each case.

The cure behavior of the epoxy resin in the presence of nanopapers was analyzed using DSC Q200 (TA Instruments). The non-isothermal DSC experiments of epoxy/nanopaper were carried out as follows: 5 g RIM 135 and 1.75 g RIM H 137 (100 : 35) were mixed homogeneously using a mini vortexer. Then, 5–10 mg of this reactive mixture was loaded into a hermetically sealed aluminum DSC pan and weighed. Then, small strips of nanopaper of the size of the DSC pan were cut using a sharp blade and were placed in the DSC pan with a pair of tweezers until the weight of the nanopapers reached 25% of the weight of the initial resin mixture. The nanopapers were then gently compacted into the epoxy resin until all the epoxy resin impregnated the nanopapers and there was no visible resin-rich area in the DSC pan. The pans were then sealed using a press and placed into the DSC for thermal measurements. The DSC was calibrated using an Indium standard. Non-isothermal experiments were performed with heating rates of 5, 10, and 20°C/min under N_2 at 50 mL/min from 0 to 300°C. A second scan with the same heating rate was carried out to determine the residual reaction heat. No residual heat was found after dynamic scanning. Hence, the final degree of conversion after non isothermal scanning was assumed to be 1.

Similarly, isothermal DSC experiments were carried out at 45, 60, and 75°C for 150 min. Then, two dynamic scans from 0 to 300°C at a heating rate of 10°C/min were carried out to measure the residual reaction heat and the glass transition temperature, respectively.

A zeta potential analyzer from Brookhaven Instruments Corp was used to measure the charge of the nanoparticles in water (neutral pH) medium. These readings were in mV and provided a direct measure of the dispersion quality of the nanoparticles in water. A minimum of three readings were taken in each case.

Surface functionalization of CNFs

In this study, three types of CNFs, namely unmodified or pristine CNFs (as received), amine modified CNFs, and carboxyl functionalized CNFs were used to prepare nanopapers. For the carboxylic functionalization, 2 g of CNFs were mixed in a 160 mL mixture of sulfuric acid and nitric acid (3 : 1 by volume). The reaction was allowed to proceed in a water bath sonicator at 50°C for 4 h. The mixture was then diluted using about 800 mL of water and centrifuged to decant all the liquid. The residue was then washed several times with water and NaOH until the pH dropped from highly acidic to neutral. Finally, the CNFs were washed with methanol to remove most of the water. The resulting slurry was then dried in a vacuum oven at 110°C for 12 h. The resulting CNFs are denoted as CNF_{COOH}.

The amine modification of the CNFs was done using PEI as the functionalizing agent. About 5g of CNFs were dispersed in 250 mL of DMF. Twenty-five gram of PEI was added to this mixture while continuously stirring it to mix the viscous polymer into the CNF/DMF mixture. The reaction mixture was continuously stirred for 96 h at 60°C. At the end of the reaction, the mixture was washed with excess water and centrifuged to dissolve and remove the un-reacted PEI. The resulting residue was then washed with 1 M hydrochloric acid (HCl) to remove DMF and remaining un-reacted PEI. The mixture was then washed with 1 M NaOH to remove the HCl. After this treatment, the functionalized CNF slurry was washed several times with water and dried in a vacuum oven at 110°C for 12 h. The resulting CNFs are denoted as CNF_{PEI}. Fourier transform infra-red spectroscopy (FTIR) was used to confirm the change in surface chemistry of the CNFs. Thermo-gravimetric analysis (TGA) was used to

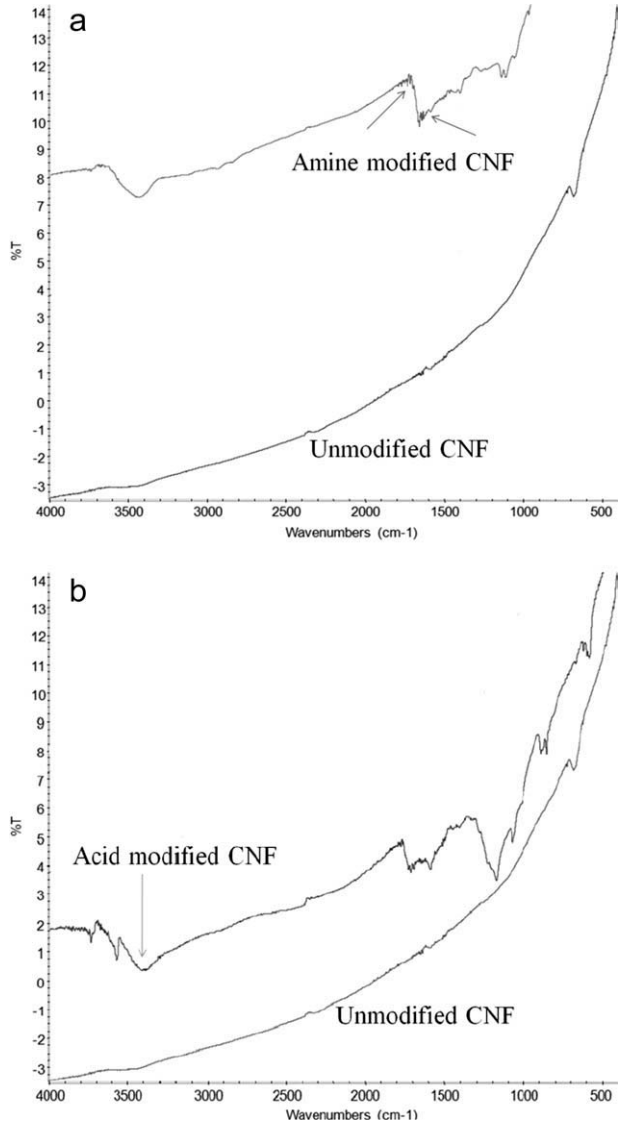

Figure 1 FTIR Spectra of (a) amine modified and (b) carboxylated CNF.

determine the weight percentage of PEI grafted from the CNFs.

RESULTS AND DISCUSSION

Nanoparticle characterization

Figure 1 shows the FTIR spectra of CNF_{COOH} and CNF_{PEI}. The strong infrared absorption at 3500 cm^{-1} for carboxylic group is well documented in the literature.[11–14] Similarly, it can be seen that there is a relatively sharp absorption at 1650 cm^{-1} for CNF_{PEI} sample indicating the presence of NH_2 groups. Figure 2 shows the TGA curves of CNF_{COOH} and CNF_{PEI} papers in comparison to the unmodified CNF paper. It can be seen that the amine functionalization method resulted in CNFs grafted with about 20 % PEI by weight. It can be seen that although the PEI layer degraded at temperatures higher than

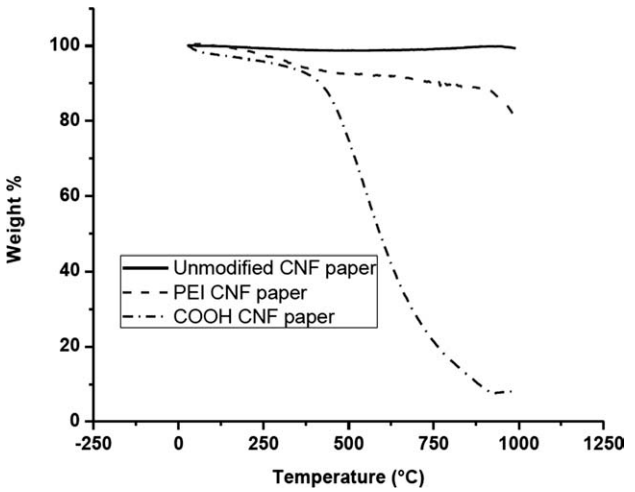

Figure 2 TGA graphs of pristine, amine modified, and carboxylated CNFs.

250°C, the underlying CNF structure remained intact. On the other hand, the structure of CNF degraded above 400°C in the case of CNF_{COOH}. This is because the strong acid treatment, while effective in imparting carboxylic functionalization on the CNF surface, also etched the structure of the CNF, making it susceptible to degradation at higher temperatures. However, this acid treatment did not result in reducing the aspect ratio of the CNFs at room temperature. The advantage of using a polyelectrolyte like PEI for the surface functionalization is that it helps in inducing a positive charge on the CNF surface in an aqueous medium. This is useful in achieving a well dispersed suspension of CNFs in water. Figure 3 shows a comparison of the dispersion efficiency of unmodified CNFs and CNF_{PEI} in water. The solutions were left to stand undisturbed for 4 h after a 30 min sonication treatment. It can be seen that unmodified CNFs (left) agglomerated and

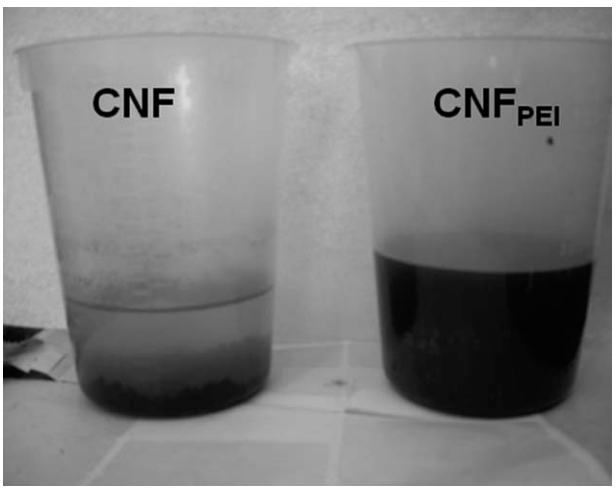

Figure 3 Dispersion of unmodified CNFs (left) and PEI-modified CNFs (right) 4 h after sonicated for 30 min.

TABLE I
Zeta Potential Values for the Three CNF Particles

Particle	Zeta potential (mV)	Standard deviation
CNF	−23.65	0.84
CNF_{COOH}	−53.03	1.61
CNF_{PEI}	+39.36	1.72

settled down, while CNF_{PEI} remained in a stable suspension. The zeta potential values for the three types of CNFs in water are presented in Table I. It can be seen that CNF_{PEI} and CNF_{COOH} have a strongly positive and strongly negative charge, respectively, in water, while unmodified CNF has a weak zeta potential leading to poor dispersion in water.

Nanopaper characterization

The bulk densities of the nanopapers were calculated by measuring the weight and volume of several samples of each type of nanopapers. The nanopaper samples were cut into rectangular strips for easy volume measurement. At least three measurements were made for each sample. Figure 4 shows the bulk density values for various nanopapers. It can be seen that surface modification helped to increase the bulk density of the nanopaper. The bulk densities of both CNF_{COOH} and CNF_{PEI} nanopapers were greater than that of the unmodified CNF paper. This is because surface modification improved the dispersion of CNFs in water, which in turn reduced agglomerates, and increased CNF uniformity and fiber-overlap during the paper formation. There was a direct correlation between the zeta potential of the CNFs and the bulk density for single layer nanopapers. CNF_{COOH} with the strongest zeta potential (−53 mV) also had the highest bulk density (0.62 g/cm^3). However, the bulk density values started to drop progressively for multilayered nanopapers. The 9 layer and 12 layer alternating CNF_{COOH}-CNF_{PEI} nanopapers had bulk densities much lower than those of the single layer CNF_{COOH} or CNF_{PEI} papers. This was unexpected as the electrostatic interaction between oppositely charged layers of the multilayered nanopaper was expected to increase the close-packing of the CNF network and hence, the bulk density. On further investigation, it was found that the first layer deposited on the filtration membrane experienced the highest vacuum force and every subsequent layer experienced a reduction in the vacuum force as the pores of the filtration membrane were covered by the CNF network. This resulted in less-effective de-bulking of the nanopaper and hence a lower bulk density. Despite a lower density, it can be seen from Figure 5 that the tensile strength values of the multilayered nanopapers were greater when compared to the single layered nanopapers. This indicates that the electrostatic forces between the positively charged layers and negatively charged layers were significant. When the tensile strength values were normalized with the bulk density values, the improvement in the strength of the nanopapers imparted by the layer-by-layer technique was even more significant.

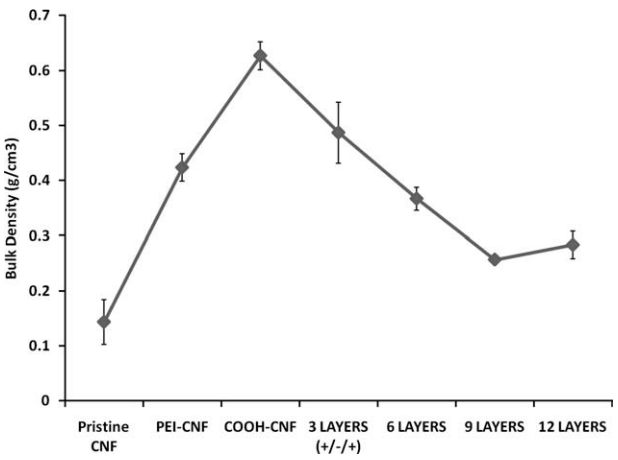

Figure 4 Bulk density values of the various nanopapers.

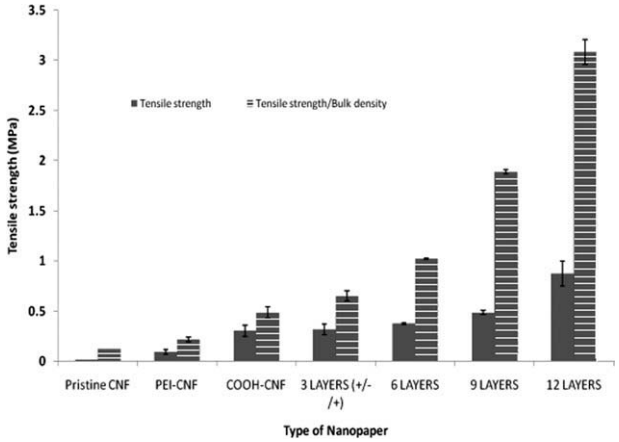

Figure 5 Tensile strength values of various stand alone nanopapers.

Effect of CNF nanopaper on cure kinetics of epoxy resin

Among all thermoset polymers, epoxy resins provide the best overall performance such as good mechanical properties, chemical resistance, and low shrinkage. Hence it is the most widely used thermoset resin. Applications include paints, electric insulators, printed circuit boards, adhesives, etc.[15] Because of its high specific strength and stiffness, it is also used as the matrix material in composites for high end applications like airplane fuselage, wind turbine blades and other high temperature aerospace

applications. The epoxy cure reaction is very important in determining the end mechanical properties of the composite.[16] On the basis of the cure reaction, epoxies can be classified into high temperature and low temperature curing systems. Many researchers have studied the cure kinetics of high temperature epoxy systems.[17,18] There have also been studies of the effect of vapor grown carbon nanofibers and carbon nanotubes on the cure kinetics of epoxy resins.[19,20] However, all these works studied the behavior of low concentration of nanoparticles dispersed in the bulk reaction phase. In this study, we investigated the effect of CNF nanopapers and their surface modification on the cure kinetics of an epoxy resin.

Figure 6 shows the non-isothermal DSC curves of epoxy RIM 135/H 137 cured at a heating rate of 10°C/min for three different cases: (1) neat epoxy resin; (2) epoxy with 25 wt % CNF paper; and (3) epoxy with 25 wt % CNF_{PEI} paper. It can be seen that although the heat of reaction was lower for both nanocomposite samples when compared to the pure epoxy, the presence of nanopapers speed up the reaction slightly. The epoxy/CNF_{PEI} paper sample had a higher accelerating effect than the epoxy/CNF paper sample. For both nanocomposite samples, the reaction started earlier and the peak exothermic temperature occurred earlier in the scanning run when compared to the neat epoxy sample. The heat of reaction and peak exothermic temperature values were 520.2 J/g and 119°C, 477.6 J/g and 115°C, and 511.8 J/g and 112°C for the neat epoxy, epoxy/CNF and epoxy/CNF_{PEI} samples, respectively.

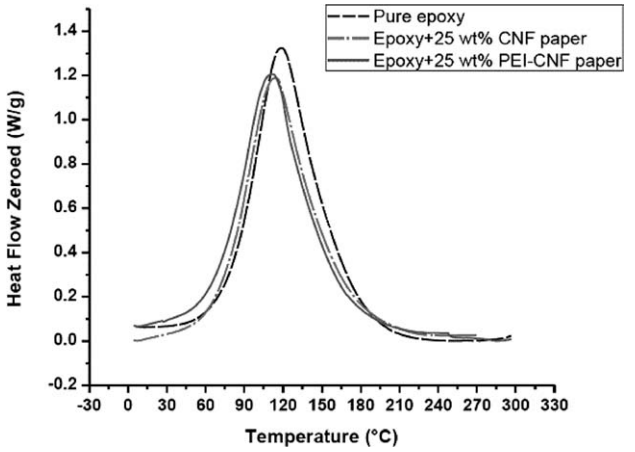

Figure 6 Non-isothermal DSC scan of pure epoxy, epoxy/CNF nanopaper composites, and epoxy-CNF_{PEI} nanopaper composites (scan rate 10°C/min).

Kinetic modeling

The basic assumption for applying DSC to the kinetic study is that the reaction rate, $d\alpha/dt$, is proportional to the measured heat flow, dH/dt, as follows:

$$\frac{d\alpha}{dt} = \frac{1}{\Delta H_{total}} \frac{dH}{dt} \tag{1}$$

where ΔH_{total} is the total enthalpy of the cure reaction measured by non-isothermal DSC scan from 30 to 300°C with a heating rate of 10°C/min.

To investigate the effect of CNF on the cure kinetics of epoxy resin, an autocatalytic model with the following generalized expression was used:

$$\frac{d\alpha}{dt} = (k_1 + k_2\alpha^m)(\alpha_f - \alpha)^n \tag{2}$$

The parameters k_1 and k_2 are the nth-order and autocatalytic rate constants, respectively, n and m are the respective reaction orders, and α_f is the final conversion. α_f equals 1 in most non-isothermal cases while the final conversion in an isothermal case can be obtained by the following equation:

$$\alpha_f = \frac{\Delta H_{total} - \Delta H_{residual}}{\Delta H_{total}} \tag{2}$$

where $\Delta H_{residual}$ is the residual heat of cure reaction after the isothermal cure, which can be measured by scanning the isothermally cured samples. In some isothermal cases, the initial conversion, α_0, was not zero since the cure process started before the cure system reached the specified isothermal temperature. Therefore, a part of reaction heat was missed at the initial stage, so we define

$$\alpha_0 = \frac{\Delta H_{total} - (\Delta H_{isothermal} + \Delta H_{residual})}{\Delta H_{total}} \tag{4}$$

where $\Delta H_{isothermal}$ is the exotherm of the cure reaction during the isothermal cure.

The rate constants, k_1 and k_2, are the temperature-dependent parameters and can be given by an Arrhenius relationship:

$$k_i = A_i \exp(-E_{a,i}/RT), i = 1, 2 \tag{5}$$

where E_a is the activation energy, R is the gas constant, T is the absolute temperature, and A is the pre-exponential factor. Equation (5) can be transformed as

$$\ln k_i = -E_{a,i}/RT + \ln A_i \tag{6}$$

By plotting $\ln k_i$ vs. $1/T$ we can determine the activation energy values to determine the specific effect of CNFs on the activation energy of the reaction.

Figure 7 shows the experimental and fit curves of the reaction rate, $d\alpha/dt$, versus conversion, α, for

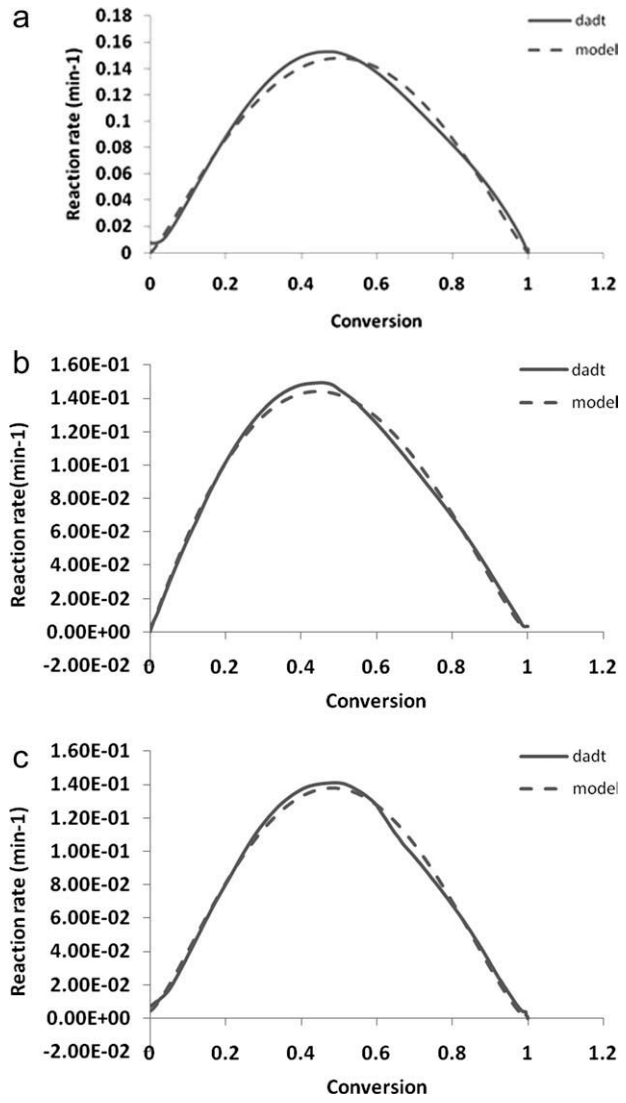

Figure 7 The experimental and fit curves of $d\alpha/dt$ vs. α for (a) pure epoxy cure, (b) epoxy-CNF paper, and (c) epoxy-CNF_{PEI} paper composite at a scanning rate of 10°C/min

epoxy-nanopaper composite systems by means of non-isothermal DSC scan at a heating rate of 10°C/min. Table II summarizes the fitting parameters. The overall order of the reaction ($m + n$) is a measure of the number of species taking part in a reaction. In most cases, epoxy reactions are assumed to have an order of two, as there are two main reacting species,

TABLE II
Reaction Rate Constants and the Corresponding Reaction Orders Obtained by Fitting Non-Isothermal DSC Data (Scan Rate of 10°C/min)

Cure system	k_1 (min^{-1})	k_2 (min^{-1})	m	n
Pure epoxy	2.12E-05	0.78	1.20	1.20
Epoxy/25 wt % CNF paper	2.00E-05	0.71	1.03	1.29
Epoxy/25 wt % CNF_{PEI} paper	4.57E-03	0.92	1.34	1.42

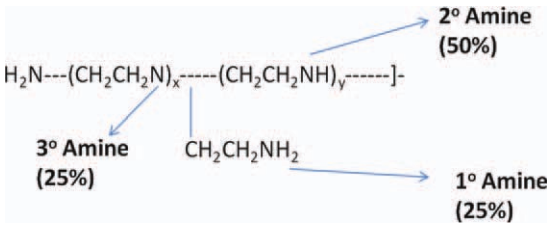

Figure 8 Structure of a typical branched PEI molecule. [Color figure can be viewed in the online issue, which is available at wileyonlinelibrary.com.]

the epoxy pre-polymer and the amine. From Table II, it can be seen that for the neat epoxy sample and the epoxy/CNF paper sample, the rounded overall order was almost the same, that is, ~ 2.

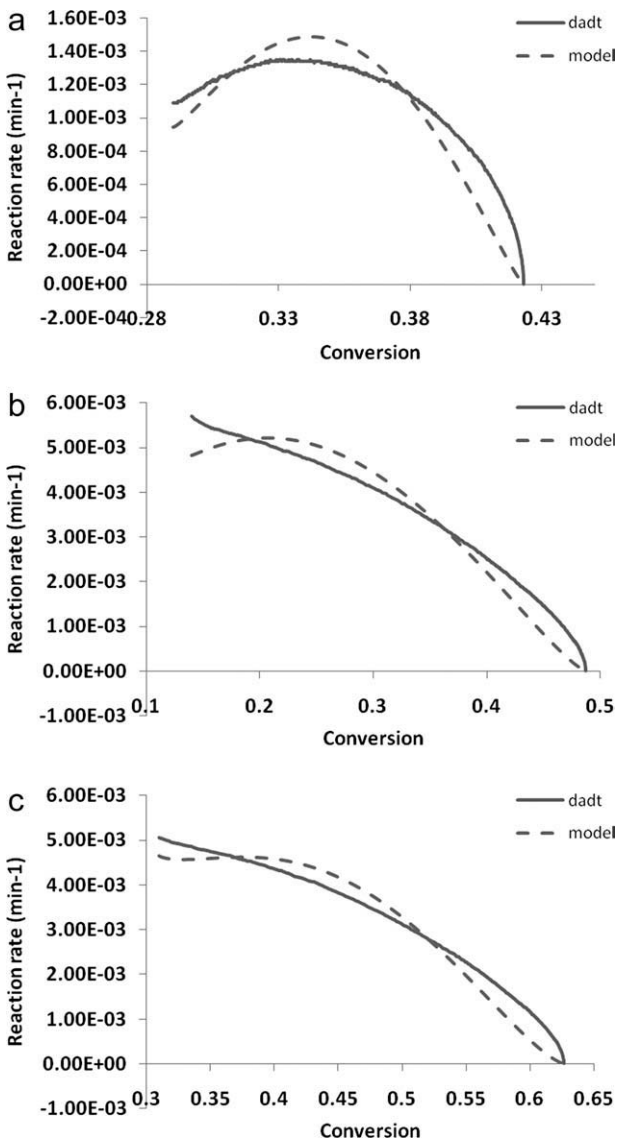

Figure 9 The experimental and fit curves of $d\alpha/dt$ vs. α for (a) pure epoxy, (b) epoxy-CNF paper system, and (c) epoxy-CNF_{PEI} paper system for isothermal cure at 45°C.

TABLE III
Reaction Rate Constants Obtained by Predicting Isothermal Cure Data at Different Temperatures Using Reaction Orders Obtained by Non-Isothermal Data Fitting

	Cure system	k_1 (min^{-1})	k_2 (min^{-1})	Conversion after isothermal cure
45°C	Pure epoxy	1.07E-02	0.68	0.42
	Epoxy/25 wt % CNF paper	1.90E-02	0.13	0.48
	Epoxy/25 wt % CNF_{PEI} paper	2.39E-02	0.36	0.62
60°C	Pure epoxy	0.01974	0.09	0.80
	Epoxy/25 wt % CNF paper	3.32E-02	0.05	0.80
	Epoxy/25 wt % CNF_{PEI} paper	3.91E-02	0.09	0.92
75°C	Pure epoxy	0.048836	0.03	0.99
	Epoxy/25 wt % CNF paper	7.10E-02	0.01	0.99
	Epoxy/25 wt % CNF_{PEI} paper	7.15E-02	0.06	1.00

However, the rounded overall order was ~ 3 for the epoxy/CNF_{PEI} paper sample. This indicates that there were more than two species taking part in the reaction. Figure 8 shows the chemical structure of the PEI molecule. A branched PEI like the one used in this study contains about 25% primary amine groups, 50% secondary amine groups and 25% tertiary amine groups. Secondary amine-epoxy reactions are the fastest and since these groups are in abundance, they might be acting as the third species in the epoxy cure reaction.

The reaction rate constant is dependent on the reaction temperature, T, whereas the reaction mechanism is independent of T. So, the reaction order values m and n obtained from the non-isothermal DSC data should be able to predict the isothermal DSC data. Figure 9 shows the experimental and fit curves of the reaction rate, $d\alpha/dt$, vs. conversion α for epoxy-nanopaper systems under isothermal cures at 45°C. Table III summarizes the reaction parameters of isothermal cure at 45, 60, and 75°C. It can be seen that the resin conversion at isothermal cures was always higher for the epoxy/CNF_{PEI} paper sample when compared to the pure epoxy and epoxy/CNF paper samples. It is important to note the increased value of k_1 within the same temperature set for the epoxy-nanopaper samples. This reaction rate constant corresponds to the initial stage of curing and the increase in k_1 implies a catalytic effect of the nanopaper on the epoxy kinetics in the early stage. According to eq. (6) and Table III, two activation energies, E_{a1} and E_{a2}, were obtained by plotting $\ln k_1$ and $\ln k_2$ against $1/T$. The activation energy values are presented in Table IV. k_1 is the nth order reaction rate constant and k_2 is the autocatalytic reaction rate constant. k_1 governs the early-stage reaction whereas k_2 affects the autocatalytic reaction after the initial stage.[21,22] From Table IV it can be seen that adding carbon nanofibers could lower both reaction activation energies.

TABLE IV
Activation Energies of Different Epoxy Cure Systems

Cure system	E_{a1} (kJ/mol)	E_{a2} (kJ/mol)
Pure epoxy	46.45	96.07
Epoxy/25 wt % CNF nanopaper	40.37	78.30
Epoxy/25 wt % CNF_{PEI} nanopaper	33.55	55.36

CONCLUSIONS

In this article, the preparation and characterization of single layer and multilayered CNF nanopapers were studied. It was shown that the dispersion of CNFs in the solvent affected the bulk density of the nanopaper, which in turn affected the mechanical strength of the stand alone nanopaper. When oppositely charged layers were mixed together to form a multilayered nanopaper, the mechanical strength of the paper increased significantly despite a loss in bulk density. This implies that the electrostatic interactions between the adjacent CNF layers were high.

The effect of CNF nanopaper and CNF_{PEI} nanopaper on the cure kinetics of an epoxy resin was investigated using both non-isothermal and isothermal DSC and the results were fitted by a modified autocatalytic cure kinetic model. It was observed that both nanopapers accelerated the cure reaction of epoxy with amine. Both activation energies of epoxy systems were decreased in the presence of the amine modified and unmodified CNF nanopapers.

References

1. Chou, T. W. Compos Sci Technol 2009, 70, 1.
2. Pham, G. T. Nanotechnology 2008, 19, 325705.
3. Gonnet, P. Curr Appl Phys 2006, 6, 119.
4. Chou, S. L. Electrochem Commun 2008, 10, 1724.
5. Guo, Z. P. J Nanosci Nanotechnol 2006, 6, 713.
6. Landi, B. J. J Nanosci Nanotechnol 2009, 9, 3406.
7. Wang, D. Nanotechnology 2008, 19, 075609.
8. Whitten, P. G. Carbon 2005, 43, 1891.
9. Wang, Z. Compos Part A: Appl Sci Manuf 2004, 35.
10. Aussawasathien, D. Macromol Symp 2008, 264, 26.
11. Jimeno, A. J Nanosci Nanotechnol 2009, 9, 6222.

12. Choi, W. J. Polym Compos 2009, 30, 415.
13. Li, S. Q. J Mater Sci 2008, 43, 2653.
14. Ahn, S. N. J Polym Sci Part A Polym Chem 2008, 46, 7473.
15. Lee, H.; Neville, K. H. Book of Epoxy Resins; New York/San Francisco: McGraw-Hill, 1967.
16. Barton, J. M. Adv Polym Sci 1985, 72, 111.
17. Opalicki, M.; Kenny, J. M.; Nicolais, L. J. Appl Polym Sci 1996, 61, 1025.
18. Perry, M. J.; Lee, L. J.; Lee, C. W. J Comp Mater 1992, 26, 274.
19. Xie, H. F. J Appl Polym Sci 2005, 96, 329.
20. Xie, H. F. J Polym Sci Part B Polym Phys 2004, 42, 3701.
21. Mijovic, J.; Fishbain, A.; Wijaya, J. Macromolecules 1992, 25, 979.
22. Palaniappan, S.; Sreedlhar, B.; Nair, S. M. Macromol Chem Phys 2001, 202, 1227.